Limnol. Oceanogr., 53(4), 2008, 1227–1241

Agent-based modeling of the complex life cycle of a cyanobacterium (*Anabaena*) in a shallow reservoir

Ferdi L. Hellweger[1]
Civil and Environmental Engineering Department, Northeastern University, Boston, Massachusetts 02115; Center for Urban Environmental Studies, Northeastern University, Boston, Massachusetts 02115

Elena S. Kravchuk
Institute of Biophysics, Siberian Branch of the Russian Academy of Sciences, Krasnoyarsk 660036, Russia

Vladimir Novotny
Civil and Environmental Engineering Department, Northeastern University, Boston, Massachusetts 02115; Center for Urban Environmental Studies, Northeastern University, Boston, Massachusetts 02115

Michail I. Gladyshev
Institute of Biophysics, Siberian Branch of the Russian Academy of Sciences, Krasnoyarsk 660036, Russia; Siberian Federal University, Krasnoyarsk 660041, Russia

Abstract

The cyanobacterium *Anabaena flos-aquae* and many other phytoplankton species have a complex life cycle that includes a resting stage (akinete). We present a new agent-based (also known as individual-based) model of *Anabaena* that includes the formation and behavior of akinetes. The model is part of a coupled Eulerian–Lagrangian model and can reproduce the main features of the observed seasonal and interannual population dynamics in Bugach Reservoir (Siberia), including an unexpectedly large bloom in a year with low nutrient concentrations. Model analysis shows that the internal loading of phosphorus (P) due to germination from the sediment bed is ~10% of the total input. However, most of the long-term nutrient uptake for *Anabaena* occurs in the sediment bed, which suggests that the sediment bed is not just a convenient overwintering location but may also be the primary source of nutrients. An in silico tracing experiment showed that most water column cells (~90%) originated from cells located in the sediment bed during the preceding winter. An in silico gene knockout experiment (akinete formation is prohibited) showed that the formation of resting stages is of critical importance to the survival of the population on an annual basis. A nutrient-reduction management scenario indicates that *Anabaena* densities increase because they are less sensitive to water column nutrient levels (because of the sediment bed source) than other species.

In lakes and reservoirs, cyanobacteria constitute a problem because they can produce surface scum blooms; low dissolved oxygen (hypoxia, anoxia); toxins; and taste, odor, and aesthetic problems, which interfere with recreation, water supply, and aquatic life (Paerl 1988; Paerl et al. 2001). To exacerbate the problem, cyanobacteria often appear unexpectedly, especially in light of decreasing phosphorus loadings, because present models predict that lower nutrient inputs would favor other species (Downing et al. 2001). In the 1980s, elimination of point sources (~$40M) and partial control of non–point source loads to Lake Delavan (Wisconsin) was followed by a massive cyanobacteria bloom (WDNR 1989). After decades of costly (~$20B) reductions in nutrient inputs to the Great Lakes, cyanobacteria are again a problem in Saginaw Bay (Lake Huron) and other locations (Vanderploeg et al. 2001). Following a large (~$650M) combined sewer overflow (CSO) reduction program, Boston was surprised in 2006 by a massive cyanobacteria bloom in its Charles River (Daley 2006). These examples highlight the complexity of cyanobacteria population dynamics and the inability of present models to predict it. Numerous physical, chemical, and biological factors and their interactions likely contribute to the observed complexity. Here we focus on one specific feature of the cyanobacteria life cycle, the formation of resting stages, which can significantly influence population dynamics (Reynolds 1972; Baker 1999).

Existing modeling approaches—Several existing phytoplankton models include cyanobacteria (Lung and Paerl 1988), but the formation and behavior of resting stages is typically not explicitly considered. However, there have been some efforts to incorporate resting stages into models. Yamamoto et al. (2002) developed a model of the dinoflagellate *Alexandrium tamarense* in Hiroshima Bay that includes encystment loss and excystment gain terms.

[1] Corresponding author (ferdi@coe.neu.edu).

Acknowledgments

We thank Jim Grover and three anonymous reviewers for their in-depth reviews and thoughtful and constructive criticism. This work was supported by the Russian Foundation for Basic Research (No. 08-04-00324).

McGillicuddy et al. (2005) present a similar model for *Alexandrium fundyense* in the Gulf of Maine. However, the cyst stage was not explicitly simulated in these models. Hense and Beckmann (2006) present a cyanobacteria model that differentiates between four life stages, including vegetative cells, vegetative cells with heterocysts, akinetes, and recruiting cells (including germlings).

The existing phytoplankton models are typically based on the traditional Eulerian or population-level approach, where population-level properties, like cell density (cells L^{-1}) or average phosphorus (P) quota (picogram (pg) $cell^{-1}$), are modified directly using differential equations. Intrapopulation variability (different life cycle stages and other properties, like size and nutrient quota) can be simulated using Eulerian cohort or stage-structured approaches (Pascual and Caswell 1997). However, as the dimensions of intrapopulation variability and complexity of processes increases this becomes more difficult, and the alternative Lagrangian or agent-based modeling (ABM, also known as individual-based modeling [IBM]) approach becomes more attractive. An agent-based model does not simulate phytoplankton using population-level variables, but individuals or agents, each with their own properties and behavior. The population-level properties emerge as a result of the cumulative behavior of the individuals. ABMs can simulate complete life cycles and adaptive behavior (i.e., akinete differentiation) to changing internal and external environmental conditions (Grimm et al. 2006). With increasing computational resources, agent-based modeling has rapidly gained popularity in ecological modeling of higher trophic levels, where the importance of intrapopulation variability and adaptive behavior has long been recognized (Grimm et al. 2006).

The purpose of this paper is to present a new agent-based model for the formation and behavior (e.g., settling, germination) of resting stage cells in phytoplankton. The cyanobacteria *Anabaena* is used as a case study, but the general model formulation should also be applicable to other species that form resting stages. The model development, including review of relevant literature and equations, is presented in the next section. Then the model application and results for Bugach Reservoir in Siberia are presented. The calibration demonstrates that the model generally captures the seasonal and interannual patterns of *Anabaena* in Bugach Reservoir, and it is then used to gain insight into the life cycle of the cyanobacterium and to evaluate management scenarios.

Model development

Overview—Spatially, the model segments the lake or reservoir into a water column and two sediment bed (aerobic and anaerobic) compartments. Horizontal gradients or differences between shallow- and deep-water sediments, which have been found to be significant for recruitment (Karlsson-Elfgren and Brunberg 2004; Kravchuk et al. 2006), are therefore not resolved. Future work may include adding this spatial dimension to the model, which could be done by expanding the existing segmentation in a manner done by Verspagen et al. (2005) or by integration with a high-resolution hydrodynamic model (Hellweger and Kianirad 2007). The model has closed element balances and tracks C and P in phytoplankton, particulate organic matter (POM), dissolved organic matter (DOM), and inorganic forms (i.e., dissolved inorganic phosphorus, DIP). A coupled Eulerian–Lagrangian approach is used, Eulerian for nonphytoplankton (e.g., extracellular nutrient) and Lagrangian for phytoplankton. This approach was used previously for nutrient–phytoplankton systems (Woods 2005). Reaction and transport processes for nonphytoplankton constituents are simulated using appropriate Eulerian equations as described in detail by Hellweger and Lall (2004). Phytoplankton are represented by discrete Lagrangian agents that go through various life cycle stages and move through the spatially structured habitat as described in detail for *Anabaena* in the remainder of this section.

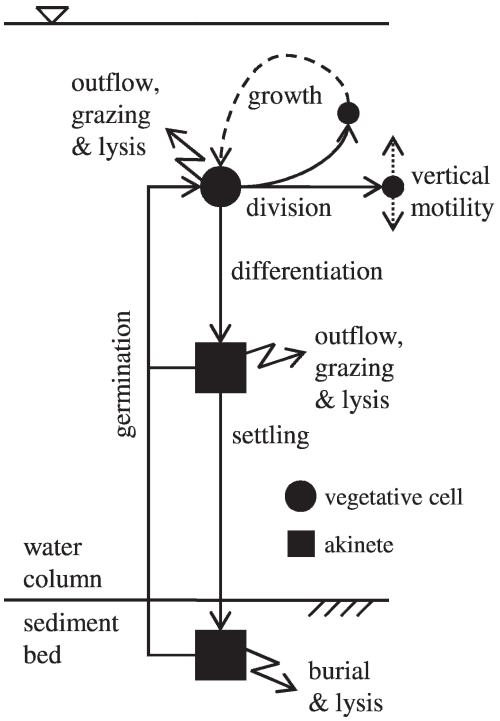

Fig. 1. Conceptual model of *Anabaena* life cycle in a lake or reservoir. Symbol size indicates cell size. The formation and function of heterocysts is not explicitly considered in the model.

Conceptual model of Anabaena *life cycle*—The conceptual model of the *Anabaena* life cycle in a lake or reservoir is outlined in Fig. 1. Here, two types of cells, vegetative and akinete, are considered. The formation and function of heterocysts, distinct cells of the filament that fix nitrogen, are not explicitly considered in this version of the model. A vegetative cell that has grown to sufficient size can either divide and form two daughter vegetative cells or differentiate into an akinete. The akinete can germinate in the water column or settle to the sediment bed and germinate there depending on the conditions (*see* below). Outflow, death (lysis), and grazing by zooplankton (although of lesser importance for filamentous cyanobacteria) can

Table 1. Algal cell state variables.

Symbol	Units	Description
z	m	depth
m	mol C cell^{-1}	size
q_P	mol P mol C^{-1}	P quota
r_i	—	life cycle stage[a]
r_T	d	life cycle time[b]

[a] *See* Fig. 2 and Table 2.
[b] Time spent in timed life cycle stages 3 or 5.

eliminate vegetative cells and akinetes. Individual cell state variables are listed in Table 1.

Cell growth and division—The biomass of an individual cell changes as a function of photosynthesis and endogenous respiration,

$$dm/dt = (\mu_P - \mu_R)\, m \tag{1}$$

where m (pmol C cell^{-1}) is the cell biomass, μ_P (d^{-1}) is the specific photosynthesis rate, and μ_R (d^{-1}) is the specific endogenous respiration rate. During the cell cycle, the cell size increases from a minimum (m_0, pmol C cell^{-1}) to twice that ($2 \times m_0$), at which point the cell divides and the size halves (Hellweger and Kianirad 2007). The photosynthesis rate is computed by multiplying a maximum rate by limitation terms for temperature, light, and phosphorus (Hellweger and Lall 2004; Prokopkin et al. 2006)

$$\mu_P = \mu_{P,MAX}\, L_T\, L_L\, L_P = \mu_{P,MAX}\, L \tag{2}$$

where $\mu_{P,MAX}$ (d^{-1}) is the maximum μ_P, L_T is the temperature limitation term, L_L is the light limitation term, and L_P is the P limitation term. An overall limitation term (L) is defined to simplify subsequent equations. The temperature limitation term is (Prokopkin et al. 2006)

$$L_T = \exp\left(-\left(\frac{T - T^0}{q}\right)^2\right) \tag{3}$$

where T (°C) is the temperature, T^0 (°C) is the optimum temperature, and q (°C) is the thermal dispersion parameter. The light limitation term is (Prokopkin et al. 2006)

$$L_L = \frac{I}{I + e + u\, I^2} \tag{4}$$

where I (W m^{-2}) is the irradiance, e (W m^{-2}) is the half-saturation constant, and u (m^2 W^{-1}) is the inhibition constant. The irradiance is computed from the surface irradiance using the light extinction formulation of Di Toro (1978), which includes dependence on phytoplankton density. Nutrient limitation is computed using the cell quota model (Droop 1968)

$$L_P = 1 - q_{0,P}/q_P \tag{5}$$

where $q_{0,P}$ (mmol P mol C^{-1}) is the P subsistence quota and q_P (mmol P mol C^{-1}) is the P quota. Cell death (lysis) and zooplankton grazing are modeled using first-order rate constants (μ_D, μ_Z, d^{-1}). The endogenous respiration and death rates are adjusted for temperature based on the common Arrhenius formulation.

The intracellular nutrient mass balance is (Hellweger and Kianirad 2007)

$$dq_P/dt = V_{DIP} - (\mu_P - \mu_R)\, q_P \tag{6}$$

where V_{DIP} (mol P mol C^{-1} d^{-1}) is the specific DIP uptake rate. The last term in Eq. 6 accounts for growth dilution, the reduction in P quota due to increase in biomass. Intracellular nutrient is not affected by cell division, because it is defined on a biomass basis. Uptake is calculated using the Michaelis–Menten model with a modification term (Thingstad 1987) to prevent unreasonably high P quotas under high nutrient and low growth conditions (i.e., in sediment bed)

$$V_{DIP} = V_{MAX,DIP}\, \frac{DIP}{K_{M,DIP} + DIP}\, \frac{q_{MAX,P} - q_P}{q_{MAX,P} - q_{0,P}} \tag{7}$$

where $q_{MAX,P}$ (mmol P mol C^{-1}) is the maximum P quota.

Vegetative → akinete transition—A review of the literature indicates that a number of factors have been found to affect akinete differentiation in *Anabaena,* including temperature (Pandey and Kashyap 1987), light (Fay et al. 1984), nitrogen (Rao et al. 1987), and phosphorus (van Dok and Hart 1996). So far, a clear mechanistic understanding of akinete differentiation has not emerged from the literature, but there appears to be consensus that it is generally triggered by unfavorable growth conditions. In fact, it has been suggested that a decreased cell division rate itself may be the trigger (Adams and Duggan 1999).

Various approaches have been used to model the formation of resting stages. Yamamoto et al. (2002) used a constant encystment rate (0.2 d^{-1}) when the P cell quota was below a threshold. McGillicuddy et al. (2005) calculated an encystment rate equal to the difference between the optimal growth rate (at local temperature, light, and salinity conditions) and the nutrient-limited growth rate. Note that those models are for the dinoflagellate *Alexandrium*. In the cyanobacteria model of Hense and Beckmann (2006), the rate of akinete formation is a function of internal energy and nutrient.

In those population-level models, resting stage formation is a rate, but for this individual-based model it is a discrete event and the rate emerges at the population level. Therefore, rather than formulating a rate, a frequency is used in this model. Akinetes are formed as an alternative to the regular cell division at a frequency (f_A), which is defined as

$$f_A = f_{A,MAX}\,(1 - L) \tag{8}$$

where $f_{A,MAX}$ is the maximum f_A, and L is the overall photosynthesis limitation term as defined in Eq. 2. Therefore, when a cell reaches the division threshold ($m \geq 2 \times m_0$) it initiates the process of akinete differentiation (instead of dividing into two vegetative daughter cells) if a random number is less than the frequency f_A. In this approach, nongrowing P-starved cells (i.e., $q_P < q_{0,P}$) do

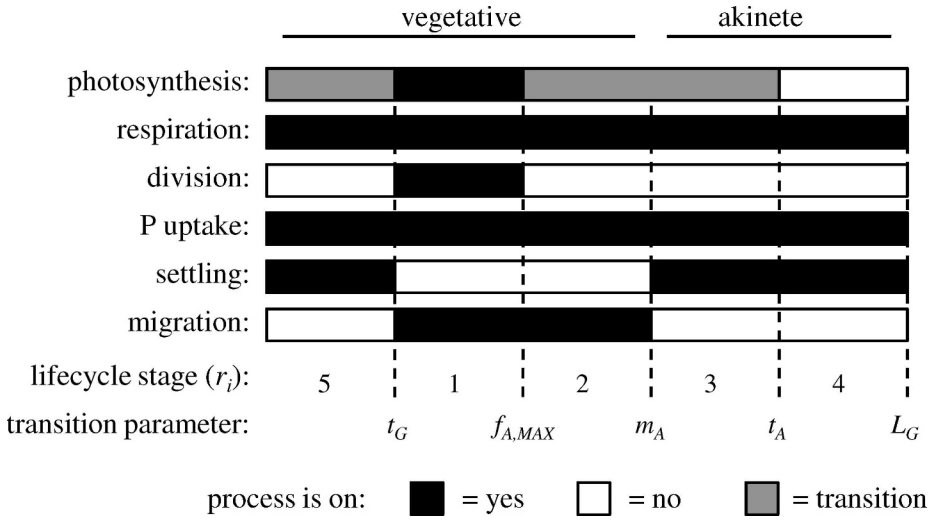

Fig. 2. Behavior of *Anabaena* for each life cycle stage (r_i). Stages 1 and 4 correspond to mature vegetative cells and akinetes, respectively. Also shown are the parameters controlling stage transitions, including the germination time (t_G), max. akinete differentiation frequency ($f_{A,\mathrm{MAX}}$), akinete size (m_A), akinete maturation time (t_A), and germination limitation (L_G). *See* Table 2.

not form akinetes, which is consistent with observations (van Dok and Hart 1996). The rate of akinete formation can be approximated as $\mu_G f_{A,\mathrm{MAX}} (1 - L) X$, where X (no. L^{-1}) is the vegetative cell density. Once the processes of akinete differentiation is initiated, it will take some time for the mature akinete to develop, and the cell remains attached to the filament for some time (Rao et al. 1987). Photosynthesis continues but decreases as the akinete matures (Fay 1969*a*). Also the fact that akinetes are typically larger than vegetative cells (Fay 1969*b*) suggests that photosynthesis continues for some time. There is no direct evidence for P uptake by akinetes, but studies show that nutrient availability affects germination (Rai and Pandey 1981), which suggests that the uptake system is active. In the model, akinete maturation and separation is modeled as a two-stage process. The five life cycle stages, as well as associated behavior and parameters controlling transitions, are illustrated in Fig. 2 and Table 2. Once akinete differentiation is initiated (r_i: 1 $\rightarrow$ 2), the cell continues to be transported (settling, migration) as a vegetative cell until it reaches a threshold size (m_A, pmol C cell^{-1}) (r_i: 2 $\rightarrow$ 3). Then, it is transported as an akinete but is not eligible for germination for a fixed time (t_A, day). The second part of the transition was found to be necessary to reproduce the observations in the application presented below. Specifically, if the feature was not included, most newly formed akinetes germinated in the water column before reaching the sediment bed. During the transition, photosynthesis decreases gradually. This is done by reducing the maximum photosynthesis rate ($\mu_{\mathrm{P,MAX}}$) in a linear fashion based on mass in the first stage

Table 2. Parameters controlling life cycle stage transitions.

Symbol	Units	Description	Value	Literature
t_G	d	Germination time	15	>1−2+[a], 2.0[b], 2.1[c]
$f_{A,\mathrm{MAX}}$	%	Max. akinete differentiation frequency	20	0.99[d], 0.6[e], 1.3[e], 5.1[f], 15[g], 49[h]
m_A	pmol C cell^{-1}	Akinete size	$20\times m_0$	$19\times m_0$[i]
t_A	d	Akinete maturation time	20	—
L_G	—	Germination limitation	0.02	$>\approx(\mu_R+\mu_D)/\mu_{\mathrm{P,MAX}}$[j]

[a] For *Anabaena circinalis* (Fay 1988), 1–2 d for signs of cell division preceding germination.
[b] For *A. circinalis* (Baker and Bellifemine 2000), for appearance of trichomes.
[c] Time required to complete 1.5 cell divisions (Adams and Duggan 1999) at $\mu = 0.5$ d^{-1}.
[d] For *A. circinalis* (van Dok and Hart 1996), $g_{A,\mathrm{MAX}} = 1.0\%$. For an exponentially growing population without loss, the frequency of akinete formation (f_A) is related to the fraction of akinetes observed in a culture (g_A) by $f_A = g_A/(1 + g_A)$
[e] For *Anabaena lemmermannii* (Olli et al. 2005), 0.6 is the maximum percentage of cells lost to sediment, 1.3 is the maximum specific production rate (2.4×10^{-3} akinete vegetative^{-1} d^{-1}), normalized to $\mu = 0.19$ d^{-1}, based on a factor of 50 population increase over 3 weeks.
[f] For *A. circinalis* (Fay et al. 1984), $g_{A,\mathrm{MAX}} = 5.4\%$. *See* footnote [d].
[g] For *Anabaena cylindrica* (Nichols et al. 1980), $g_{A,\mathrm{MAX}} = 18\%$. *See* footnote [d].
[h] For *Anabaena doliolum* (Pandey and Kashyap 1987), $g_{A,\mathrm{MAX}} = 95\%$. *See* footnote [d].
[i] Akinete size for *A. cylindrica* (Fay 1969*b*), from cell volume (Converted using $m_{\mathrm{AVE}} = 2 \ln(2)\, m_0$; Hellweger and Kianirad 2007). Model akinete size can be larger because growth can continue through stage 3.
[j] The value corresponds to zero net growth, when photosynthesis is balanced by respiration and death (omitting grazing, settling, and outflow losses).

($1.0 \rightarrow 0.5$ as m: $2 \times m_0 \rightarrow m_A$) and time in the second stage ($0.5 \rightarrow 0.0$ as r_T: $0 \rightarrow t_A$). Respiration and P uptake are the same for all life cycle stages.

Akinete → vegetative transition—As with akinete formation, the literature indicates that a number of factors have been found to affect akinete germination in *Anabaena,* including temperature (Baker and Bellifemine 2000), light (Fay 1988), nitrogen (Rai and Pandey 1981), and phosphorus (Rai and Pandey 1981). Again, no consistent mechanistic understanding emerges from the literature, but there is a general agreement that favorable growth conditions trigger akinete germination.

As with resting stage differentiation, various modeling approaches have been used to simulate the germination of resting stage cells. Yamamoto et al. (2002) used a light-dependent excystment rate. McGillicuddy et al. (2005) calculated an excystment rate based on an endogenous clock (time of year), temperature, and light. Again, those models are for the dinoflagellate *Alexandrium*. In the model of Hense and Beckmann (2006), the transition is again based on threshold values for internal energy and nutrients.

In this model, the same general approach used for akinete differentiation is adopted for germination. Akinetes germinate when conditions are favorable for growth, specifically when the overall photosynthesis limitation term (L) is greater than a threshold (L_G). In the sediment bed, germination occurs within a specified depth (H_G, m), where the light intensity is assumed to be equal to that at the sediment bed surface. Once germination is initiated, it takes some time before mature vegetative cells develop. Typically a few cell divisions occur within the akinete envelope before germlings emerge (Adams and Duggan 1999; Baker and Bellifemine 2000), and then it may still take some more time before mature trichomes develop. In this model, the transition from akinete to vegetative cell is assumed to require a maturation time (t_G, day). The akinete germinates first (r_i: $4 \rightarrow 5$) and then turns into a mature vegetative cell (r_i: $5 \rightarrow 1$) (*see* Fig. 2). During the transition, the cell is transported (settling, migration) as an akinete. The photosynthesis rate increases gradually by increasing the maximum photosynthesis rate ($\mu_{P,MAX}$) in a linear fashion based on time ($0.0 \rightarrow 1.0$ as r_T: $0 \rightarrow t_G$). As a result, the cells undergo an initial period of growth on the sediment bed. This is consistent with observations of Karlsson (2003), who found that after germination, *Gloeotrichia echinulata* undergo a period of growth on the sediment bed before the filaments develop gas vacuoles and migrate up into the water column.

Transport—In the water column, settling, vertical migration, vertical mixing, and outflow transport processes are included. Settling is simulated using a constant settling velocity (v_S, m d^{-1}). Some cyanobacteria, including *Anabaena,* exhibit vertical motility by buoyancy regulation via gas vesicles (Head et al. 1999*a;* Westwood and Ganf 2004). Detailed mechanistic models of buoyancy and vertical migration in cyanobacteria exist and could be incorporated into this model (Howard 2001). However, for the present model structure (no vertical nutrient gradient), parameterization (no light inhibition), and application (shallow reservoir, average depth 2 m), the optimum depth is always at the surface. Therefore, vertical motility is included in a simplified manner by assigning a constant upward vertical migration velocity (v_M, m d^{-1}). Vertical mixing is included using a random walk component, where $\Delta z = (2 \times E_Z \times \Delta t)^{0.5} \times R$, where Δz (m) is the vertical displacement, E_Z (m^2 s^{-1}) is the vertical dispersion coefficient, Δt (s) is the time step, and R is a random number drawn from a standard normal probability distribution (mean = 0, standard deviation = 1) (Chapra 1997). In the sediment bed, burial and vertical mixing transport processes are included.

Implementation—The model, called *iAlgae,* is a modified version of the public-domain *OldLace* lake modeling framework (Hellweger and Lall 2004). The major modifications include simulating algae as discrete individual agents using the methodology described by Hellweger and Kianirad (2007) and Hellweger (2008) and incorporating the complex life cycle processes of *Anabaena* as described above.

The differential equations are solved using an explicit finite differences approach (Chapra 1997). In the coupled Eulerian–Lagrangian approach, when calculating mass transfer from concentration to agent pools, the cumulative effect of all the agents has to be accounted for. This is illustrated in the following mass balance equation for DIP:

$$V \frac{d\mathrm{DIP}}{dt} = \sum_{\text{agents}} [-V_{\mathrm{DIP}}\, m\, S_R] + k_{\mathrm{DOP}}\, \mathrm{DOP}\, V \qquad (9)$$

where V (m^3) is the segment volume, V_{DIP} (mol P mol C^{-1} d^{-1}) is the specific DIP uptake rate, m (pmol C $cell^{-1}$) is the cell size, S_R (cell super-$cell^{-1}$) is the super-individual upscaling factor (discussed further below), and k_{DOP} (d^{-1}) is the dissolved organic phosphorus (DOP) mineralization rate constant.

The number of individual cells in a lake or reservoir can be very large, making it unfeasible to simulate every single cell; the model therefore simulates a smaller number of representative individuals. This is known as the "super-individual" approach originally developed by Scheffer et al. (1995). Hellweger (2008) presented a modification of that method for spatially explicit models where the number of agents in each spatial segment, as opposed to globally, is maintained within a specified range. Here, that method is further expanded to consider the number of agents in each life cycle stage. That means the model will, for example, always have 500–1,000 *Anabaena* akinetes in the sediment bed layer. As in the method of Hellweger (2008), each agent has its own upscaling factor (S_R) specifying how many cells it represents, and that number changes during the simulation. The minimum number of agents required is a function of the intrapopulation variability and is established by gradually increasing it until the results are no longer sensitive to the seed value of the random number generator. In the application presented subsequently $(5–10) \times 10^3$ agents are used to represent about 1.4×10^{18} real *Anabaena* cells, corresponding to an upscaling factor of $(1.4–2.8) \times 10^{14}$.

Table 3. Algae parameters.

Symbol	Units	*Anabaena*		Others	
		Value[a]	Literature[b]	Value	Literature
v_S	m d^{-1}	v, 0.0; a, 0.3	*see* Others column	0.02	0.0–17[c]
v_M	m d^{-1}	v, 1.0; a, 0.0	0.2–10[d]	—	—
m_0	pmol C $cell^{-1}$	0.82	0.39[e], *0.82*[f], 0.98[g]	1.0	10^{-8}–10^{11} [c]
$\mu_{P,MAX}$	d^{-1}	0.75	0.4–1.1[h], *0.60*[i], 0.66[j], 0.94–1.3[k], *0.95–1.3*[f], *0.99*[l]	1.8	1.8 (1.5–2.5)[m]
T^0	°C	22	*18–22.5*[n], *22*[i], 22–24[o]	17	6–18[p]
q	°C	5	*5*[i]	10	—
e	W m^{-2}	25	*25*[i]	15	—
u	m^2 W^{-1}	0.001	*0.001*[i]	0.001	—
$q_{0,P}$	mmol P mol C^{-1}	3.5	0.77[q], 1.1[k], 1.2, 2.3[r], 1.3[s], *3.5*[t]	2.0	0.3–8[u] (Redfield = 9.4)
μ_R	d^{-1}	—	v: 0.056[j], v/a: 100[v]	0.05	range, 0.01–0.5; typical, 0.1–0.2[w]
θ_R	—	—	*see* Others column	1.08	1.08[w]
H_G	μm	20	—	—	—
$V_{MAX,DIP}$	mol P mol C^{-1} d^{-1}	0.0012	*0.13–1.3*[t], 0.014–0.072[s], 0.60–0.68[x]	0.006	0.0016–1.3[y]
$K_{M,DIP}$	μmol P L^{-1}	2.0	0.06[s], *0.96–2.8*[t], 1.1–9.5[x]	2.0	0.90–16[y]
$q_{MAX,P}$	mmol P mol C^{-1}	$20\times q_{0,P}$	*see* Others column	$10\times q_{0,P}$	$5-13\times q_{0,P}$[u], $6.8-20\times q_{0,P}$[z]
μ_D	d^{-1}	vw, 0.06; aw, 0.0006; s, 0.0055	v, *0.0082–0.10*[l], *0.048*[i], 0.056[j]; v/a, 100[v]	0.06	—
θ_D	—	w, 1.08; s, 1.2	—	1.08	—
μ_Z	d^{-1}	0.0	—	0–0.4[A]	0.03–0.06[B]

[a] v, vegetative; a, akinete; w, water column; s, sediment bed; where different.
[b] Literature values for *Anabaena flos-aquae* or *Anabaena* in Bugach Reservoir or Krasnoyarsk Reservoir (close to Bugach Reservoir) are in italics.
[c] Wetzel (2001), p. 346–7, p. 335.
[d] For *Anabaena circinalis* (Westwood and Ganf 2004).
[e] From m_{AVE} = 0.542 pmol C $cell^{-1}$ for *Anabaena variabilis* (Shuter 1978). Converted using $m_{AVE} = 2\ \ln(2)\ m_0$; Hellweger and Kianirad (2007).
[f] For *Anabaena flos-aquae* (Rhee and Lederman 1983). Converted using $m_{AVE} = 2\ \ln(2)\ m_0$; Hellweger and Kianirad (2007), μ_{MAX}.
[g] From m_{AVE} = 1.36 pmol C $cell^{-1}$ for *Anabanea* sp. (Oh et al. 1991). Converted using $m_{AVE} = 2\ \ln(2)\ m_0$; Hellweger and Kianirad (2007).
[h] For various *Anabaena* species (Tang et al. 1997), μ_{MAX}.
[i] For *Anabaena* in Krasnoyarsk Reservoir, Siberia (Prokopkin et al. 2006), μ_{MAX}, mg wet L^{-1} calculated assuming 40% C, 10% dry.
[j] For *A. circianalis* (Westwood and Ganf 2004). Value for μ_R and μ_D is "loss rate."
[k] For *Anabaena* sp. (Oh et al. 1991), μ_{MAX}.
[l] For *Anabaena flos-aquae* (Lee and Rhee 1999), μ_{MAX}.
[m] Thomann and Mueller (1987), p. 420.
[n] For *Anabaena flos-aquae* (Tang et al. 1997).
[o] For *A. circinalis* (Fay 1988).
[p] Range of values used in applications by HydroQual (1998, 2001).
[q] For *Anabaena wisconsinense* (Healey 1982) converted assuming 40% C.
[r] For *A. variabilis* (Shuter 1978).
[s] For *Anabaena planctonica* (Smith and Kalff 1982) converted assuming 10% dry, 40% C.
[t] For *Anabaena flos-aquae* (Healey 1982) converted assuming 40% C.
[u] Various species (Sommer 1998).
[v] Ratio of vegetative to akinete mortality in model of Hense and Beckmann (2006).
[w] Respiration and excretion, Chapra (1997), p. 614.
[x] For *A. variabilis* (Healey 1982) converted assuming 40% C.
[y] Range of values summarized by Hellweger et al. (2003), Table 3.
[z] Various species (Morel 1987).
[A] The zooplankton grazing rate varies on a monthly basis.
[B] Range used in model of HydroQual (1998).

When using the super-individual approach, mortality and outflow can be simulated in one of two ways (Scheffer et al. 1995; Hellweger 2008). Consider, for example, grazing mortality at a rate of μ_Z (d^{-1}). One option is to compute the corresponding probability of mortality in a given time step ($\mu_Z \times \Delta t$), and if a random number from a uniform distribution between 0 and 1 is less than the probability, the agent is eliminated. Another option is to apply the rate to the representative number (S_R). That means the agent remains active, but its representative number is reduced ($S_R = S_R - S_R \times \mu_Z \times \Delta t$). In this model, grazing mortality and outflow are implemented in the second manner.

Aside from the random walk transport and akinete differentiation processes, the model described so far is purely deterministic. However, there is natural internal variability, and not accounting for it can lead to unrealistic numerical synchronization effects (Hellweger and Kianirad 2007). Therefore, internal variability is introduced using the method of Kreft et al. (1998). Upon division, model coefficients (e.g., $\mu_{P,MAX}$, $q_{0,P}$, …) are drawn from a normal distribution with user-specified mean (*see* Table 3) and coefficient of variation (a value of 0.10 is used in this application), truncated to $\pm 2\ \sigma$ and ≥ 0 to prevent unrealistic values (e.g., negative $q_{0,P}$).

Model application

Study site—The model is applied to *Anabaena flos-aquae* in Bugach Reservoir (Siberia). Detailed descriptions of the reservoir ecosystem are given elsewhere (Kalachova et al. 2004). Briefly, the reservoir is situated (56°03′N, 92°43′E) in the vicinity of Krasnoyarsk City on the Bugach River, a secondary tributary to the Yenisei River. The reservoir has surface area of about 0.32 km^2; maximum and mean depths of 7 m and 2 m, respectively; and a hydraulic residence time of about 160 d. Bugach Reservoir is eutrophic, with annual summer cyanobacteria blooms, and is used for recreation and fishing.

Model input—For the model application, the phytoplankton community is divided into two subpopulations, *Anabaena* and others (all other species). Respiration of *Anabaena* is not explicitly considered; rather it is lumped in with the photosynthesis (i.e., net growth). Values for the phytoplankton parameters are presented and compared with literature values in Tables 2 and 3. The values for all other parameters (e.g., particulate organic P hydrolysis rate constant) are as in Hellweger and Lall (2004), except for the sediment bed thickness, which was taken to be 1 cm to be consistent with the field data. Parameter values are generally consistent with those presented in the literature, where available, with some exceptions. The germination time (t_G) is higher than the values reported in the literature, but those are for laboratory experiments where the germination conditions (light, temperature) may have been better than in the field. The maximum uptake rate ($V_{MAX,DIP}$) is significantly lower than those reported in the literature. A possible explanation is that not all DIP is available for uptake. Higher trophic levels are not explicitly simulated, and the effect of grazing on non-*Anabaena* phytoplankton is accounted for with a monthly variable grazing rate (μ_Z). Assigning zooplankton grazing in this manner limits the utility of the model to simulate different conditions, under which zooplankton density may change. However, no grazing loss is included for *Anabaena,* and for the purpose of testing the *Anabaena* model, this is therefore not considered a limitation. Temperature is varied seasonally, and irradiance is varied seasonally and attenuated under ice (*see* Fig. 3a). The diel light cycle is not resolved by the model. The P inflow concentration is assigned 24, 8, and 8 μmol P L^{-1} in years 1, 2, and 3, respectively, based on observed water column concentrations (*see* Fig. 3c). Prokopkin et al. (2006) used a constant value of 16 μmol P L^{-1} for 1997–2002. All other forcing functions are assigned temporally constant. The data for the model calibration are from Kravchuk et al. (2006).

Model results

Calibration to conventional parameters—The observed and simulated conventional water quality parameters are presented in Fig. 3. The simulated DIP concentrations are very high in the winter, and no data are available to confirm them (Fig. 3c). However, lake winter DIP concentrations are typically higher (Rigler 1964), and similar differences between ice and ice-free conditions have been observed for other waterbodies (e.g., 2 → 0.1 μmol P L^{-1}; Vadstein et al. 1988). Also, no sediment P data are available, but the simulated concentration (average 5.7 mg P g^{-1}) is within the range of measurements for other waterbodies (2.4–10 mg P g^{-1}; Bortleson and Lee 1974). Chlorophyll *a* exhibits strong spring and fall blooms in year 1 and less productivity in years 2 and 3 (Fig. 3d). The model generally reproduces this trend as a result of the interannual pattern in DIP loading and resulting concentration (Fig. 3c). In addition, biomanipulation performed in the reservoir during the simulation period (Prokopkin et al. 2006), which is not accounted for in the model, may have led to interannual variability and may contribute to disagreement between the model and data.

Calibration to Anabaena *densities*—The observed and simulated *Anabaena* densities are presented in Fig. 4, which demonstrates that the model reproduces the general seasonal and interannual patterns in Bugach Reservoir. At the beginning of the simulation, the population resides as akinetes in the sediment bed. The density gradually decreases as a result of death and burial into the deeper sediment. In the spring, the growth conditions improve, and the cells germinate and enter the water column, where they grow. The density is relatively high as a result of the higher DIP concentration in that year. Akinetes start forming in the water column at an increased rate as the growth conditions worsen, and as they settle, their density in the sediment bed increases. As a result of the higher productivity in the first year, the akinete sediment density at the beginning of year 2 is higher. This causes a more pronounced bloom. However, because the DIP concentration is lower, that bloom cannot be sustained for long, resulting in lower sediment bed akinetes at the beginning of year 3. As a result, the bloom is lower in year 3, and because the DIP concentration is also low, it dies off relatively quickly. Although the model reproduces the general patterns of the *Anabaena* life cycle, there are some discrepancies. The model predicts that essentially all sediment bed akinetes germinate in year 1, which is not supported by the data. This is due to relatively good growth conditions at the sediment bed surface for a sufficiently long time to allow all akinetes to get mixed up to the sediment bed surface, considering the particle mixing and assigned germination depth. However, the model reproduces the partial germination of the sediment bed akinete population in year 2. Another discrepancy is that the model predicts significant secondary peaks in water column densities in years 2 and 3. However, the data also show secondary peaks, even though they are not as pronounced and clearly visible at the scale of the figure. The root mean squared error (RMSE) for the water column vegetative, water column akinete, and sediment bed akinete predictions are 36×10^6 cells L^{-1}, 0.25×10^6 cells L^{-1}, and 0.13×10^6 cells cm^{-2}, respectively. The model is able to capture the influence of resting stages on the population dynamics. The higher bloom in year 2, despite the lower nutrient concentration, highlights the importance of the resting stage and the utility of the model. A model that does not account for this feature would not have been able to predict this behavior.

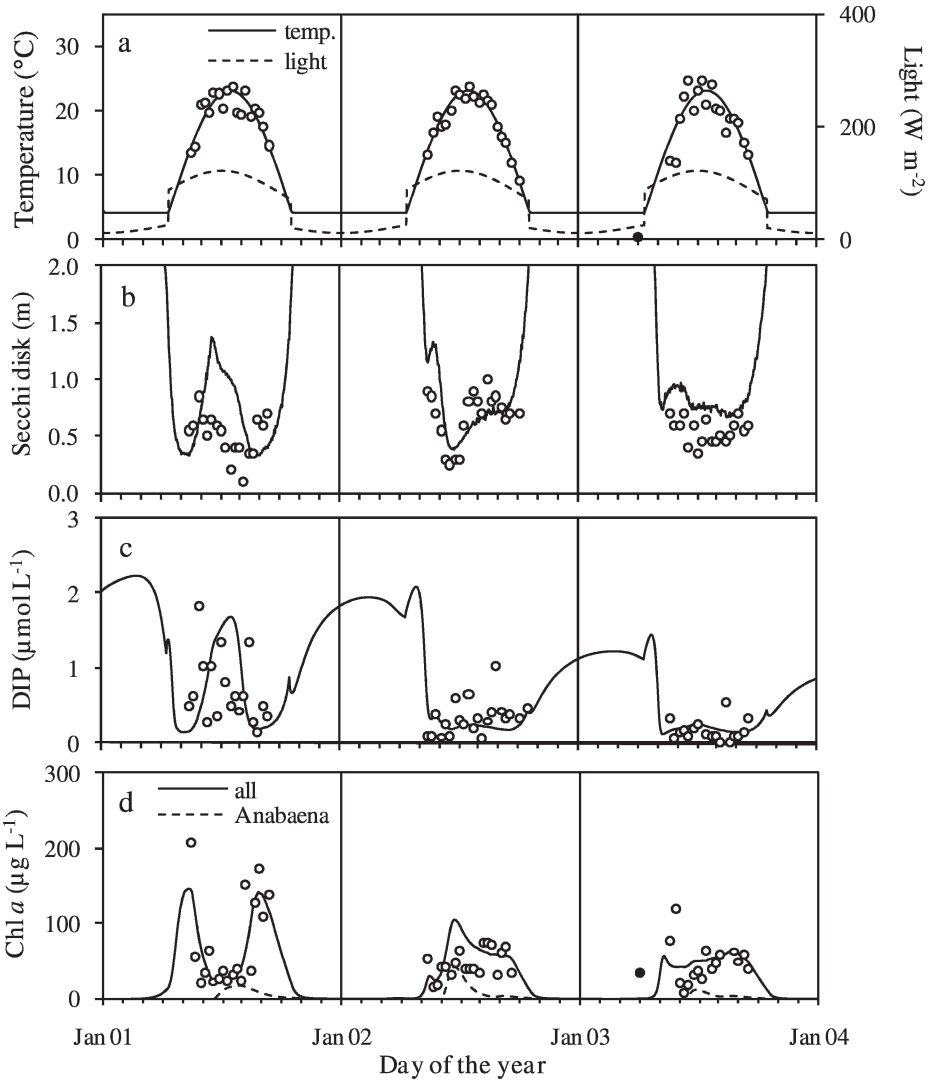

Fig. 3. Model calibration to (a) temperature and light, (b) Secchi disk transparency, (c) dissolved inorganic phosphorus (DIP), and (d) chlorophyll *a*. Solid and dashed lines are model predictions, and symbols are data from Kravchuk et al. (2006). Closed symbols correspond to one under-ice sample. Model extinction coefficient (K_e) was converted to Secchi disk depth (z_s) using $K_e = 1.8/z_s$ (Thomann and Mueller 1987). Model phytoplankton C was converted to chlorophyll *a* using 65 μg C μg Chl a^{-1}.

Life history of individuals—It is instructive to examine the history of an individual cell, presented in Fig. 5. The cell starts in the sediment bed (depth (z) $\approx$ 2 m, Fig. 5a). When the temperature and light (nutrients are in excess in the sediment bed) increase, the cell germinates, which is associated with a significant size reduction (m: $\sim m_A \rightarrow m_0$, Fig. 5b). The cell spends some time (t_G) on the sediment bed and then enters the water column, where its position changes because of vertical dispersion and migration. The cell performs photosynthesis, which is associated with a decrease in cell quota (q_P, Fig. 5c) and undergoes a number of divisions, which are associated with sudden drops in size. Later, the cell initiates akinete differentiation, grows to a full akinete, and settles back to the sediment bed. Figure 5d shows the life cycle stage index for the cell (*see* Table 1 and Fig. 2). In year 2, the cell germinates but does not revert back to an akinete; rather it overwinters in the water column. In year 3, it differentiates to an akinete and settles to the sediment bed.

Internal loading due to germination—Akinetes that germinate in or on the sediment bed and migrate to the water column carry with them P, which is a form of internal loading. Barbiero and Welch (1992) found P input to Green Lake, Seattle, due to migrating *G. echinulata* to be 73 (1989) and 7.7 (1990) μmol P m^{-2} d^{-1}. Pettersson et al. (1993) estimated P input to Lake Erken due to migrating *G. echinulata* to be 81 μmol P m^{-2} d^{-1}. Barbiero and Kann (1994) found P input to Agency Lake, Oregon, due to migrating *Aphanizomenon flos-aquae* to be 110 μmol P m^{-2} d^{-1}. Head et al. (1999*a*) found a net upward flux in the water column of Cauldshiels Loch of approximately

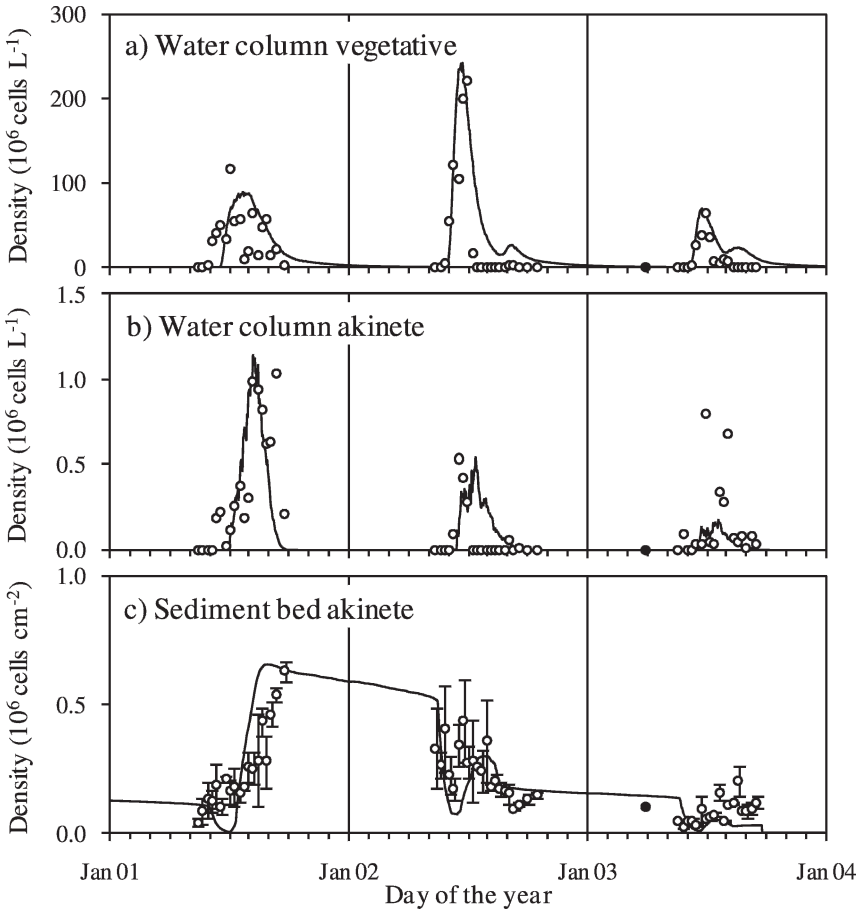

Fig. 4. Model calibration to *Anabaena flos-aquae*. (a) Vegetative cells in the water column, (b) akinete (resting stage) cells in the water column, and (c) akinetes in the sediment bed, ±1 SE (top 1 cm). Solids lines are model predictions and symbols are data from Kravchuk et al. (2006). Closed symbols correspond to one under-ice sample.

65 μmol P m^{-2} d^{-1} as a result of vertical migration of various species of cyanobacteria, including *Anabaena*. The model predicts that the P flux due to migrating *Anabaena* in Bugach Reservoir during the main germination period (June) is 27, 241, and 56 μmol P m^{-2} d^{-1}, for years 1, 2, and 3, respectively (Fig. 6a). This flux is consistent with those from the literature. Figure 6b presents the sources and sinks of P to and from the water column over the 3-yr simulation period. The internal loading to Bugach Reservoir due to *Anabaena* germination constitutes ~10% of the total P input.

Water column vs. sediment bed uptake—Anabaena can absorb nutrients in the water column and in or on the sediment bed. Several studies for other species (*G. echinulata, Aphanizomenon flos-aquae*) have shown that the P content of sediment bed or newly recruited cells was larger than that of water column cells (Pettersson et al. 1993; Barbiero and Kann 1994; Karlsson 2003). The nutrient uptake does not have to occur within the sediment bed layer when the cells are in the akinete form but can also occur on the sediment bed following germination during the initial period of growth (Karlsson 2003). In the model, the total uptake of P by *Anabaena* in the sediment bed is six times higher than that in the water column, suggesting that the sediment bed is not only a convenient overwintering compartment, but also the predominant source of nutrients.

Overwintering location—There is continuing debate about the location of the overwintering compartment for *Anabaena flos-aquae*. Specifically, some studies find that the population overwinters in the water column (Head et al. 1999*b*), and others find that it overwinters in the sediment bed (Baker 1999). To investigate the importance of akinete formation in Bugach Reservoir, we estimate the number of water column cells that originate from the sediment bed (vs. those that overwintered in the water column). Basing this type of estimate on observations alone is difficult because there is continuous growth, and recently germinated cells may grow faster (due to higher P stores) than those originally resident in the water column. Consider the density of akinetes in the sediment bed of Bugach Reservoir at the end of year 1. The density 0.5×10^6 cells cm^{-2} corresponds to 2.5×10^6 cells L^{-1} over a depth of 2 m, which is insignificant when compared with the observed

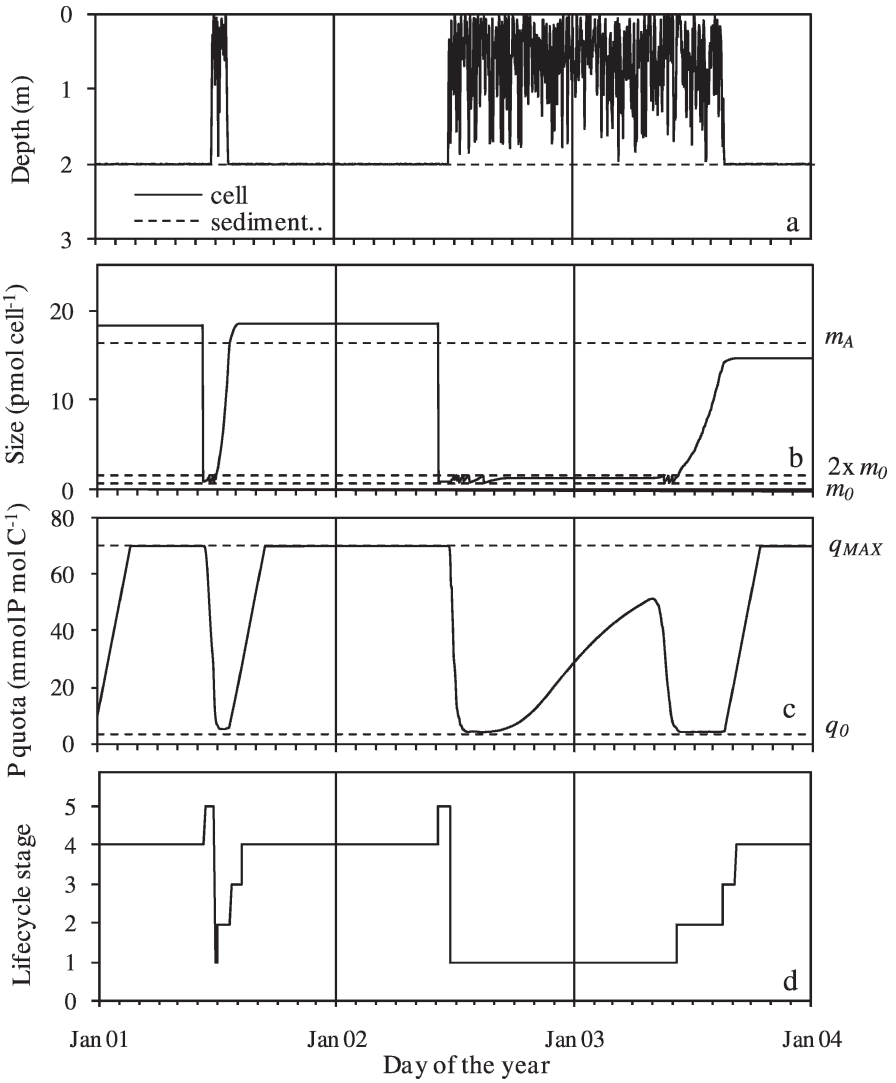

Fig. 5. History of an individual *Anabaena* cell lineage (solid line). (a) Depth (z), (b) size (m), (c) P quota (q_P), and (d) life cycle stage (r_i, *see* Table 1). Only one of two daughter cells is followed after division.

water column density (Fig. 4). However, if it is considered that the sediment akinetes are 10× larger and have 10× higher P quota, then this (after a number of cell divisions) corresponds to 250×10^6 cells L^{-1}, which is comparable to the observed water column density in year 2. To understand the importance of akinete formation for *Anabaena* in Bugach Reservoir, we performed an in silico tracing experiment, where we tagged cells that are located in sediment bed at the beginning of each year. The marker is passed across generations, which constitutes the tracing. Figure 7a presents the density of tagged cells in the water column. Note that the results for year 1 should be dismissed because they are dictated by the initial conditions, which specify all cells to be in the sediment bed. The results for years 2 and 3 illustrate that most of the water column population originates from cells that were in the sediment bed in the previous winter. At the time of peak density in years 2 and 3, 90% and 84%, respectively, of the cells in the water column originate from the sediment bed.

Role of resting stages—Although it is reasonable to assume that akinete formation is generally beneficial for *Anabaena,* the exact role of this trait at the population level remains unclear. Is it a mechanism for overwintering and absorbing nutrients in the sediment bed on an annual basis? Or, do resting stages represent adaptation to and protection from (in the form of an insurance policy) crash situations (floods, droughts) only? To investigate this, we performed a diagnostic simulation where akinetes are not allowed to form, essentially an ecosystem-scale gene knockout experiment conducted in silico. Although the formation of akinetes is prohibited, for consistency with the base case, the simulation starts with the akinete population in the sediment bed (i.e., the germination gene is not knocked out). The model predicts that the *Anabaena* water column vegetative cell density in year 1 increases (Fig. 7b), which makes sense, because when no akinetes form, more vegetative cells form. The difference between the "knockout" and "wildtype" (base case) can be interpreted as an

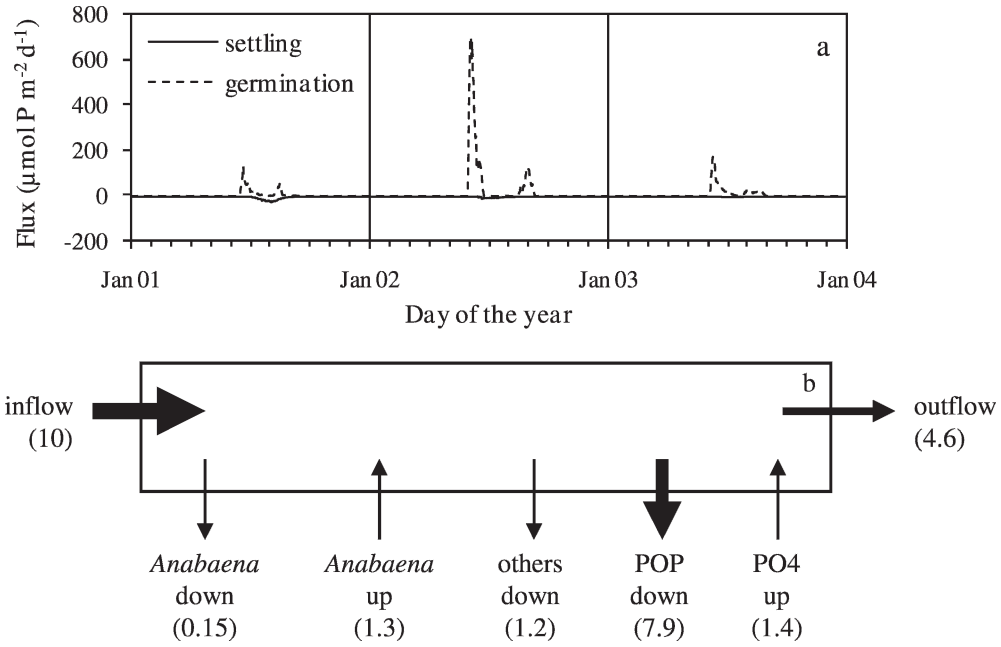

Fig. 6. Internal loading due to germinating akinetes. (a) P flux due to settling and germinating *Anabaena* in Bugach Reservoir. (b) P mass balance for the water column. Values in brackets are averages over the 3-yr simulation period in kmol P yr^{-1}. Arrow thickness is proportional to flux magnitude. The net loss over the 3-yr period is 1.0 kmol P yr^{-1} and corresponds to a decrease in water column total P concentration of 1.6 μmol L^{-1}.

investment into the survival of the population. Because the knockout population didn't put anything "in the bank," it becomes extinct within 1 yr. Based on the results presented above, the main benefit of akinetes may be nutrient uptake in the sediment bed. Therefore, according to the model, for *Anabaena* in Bugach Reservoir, the formation of akinetes is of critical importance for the survival of the population on an annual basis.

Evaluating management actions—Potential management actions for cyanobacteria are numerous and include algicides, external (point sources and non–point sources)

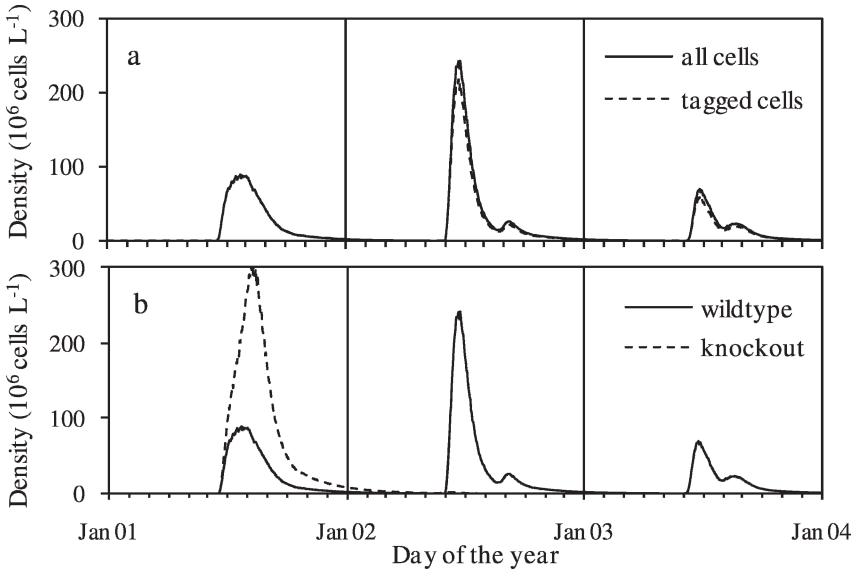

Fig. 7. Overwintering location and role of akinetes. (a) Tagging cells to determine the overwintering location. Cells in the sediment bed are tagged at the beginning of each year. Figure shows densities of all and tagged cells. (b) Preventing akinete differentiation to investigate the role of akinetes. "Wildtype" simulation is the base case presented in Fig. 4. "Knockout" simulation is same with $f_{A,\mathrm{MAX}} = 0$. Both panels show *Anabaena* vegetative cells in water column.

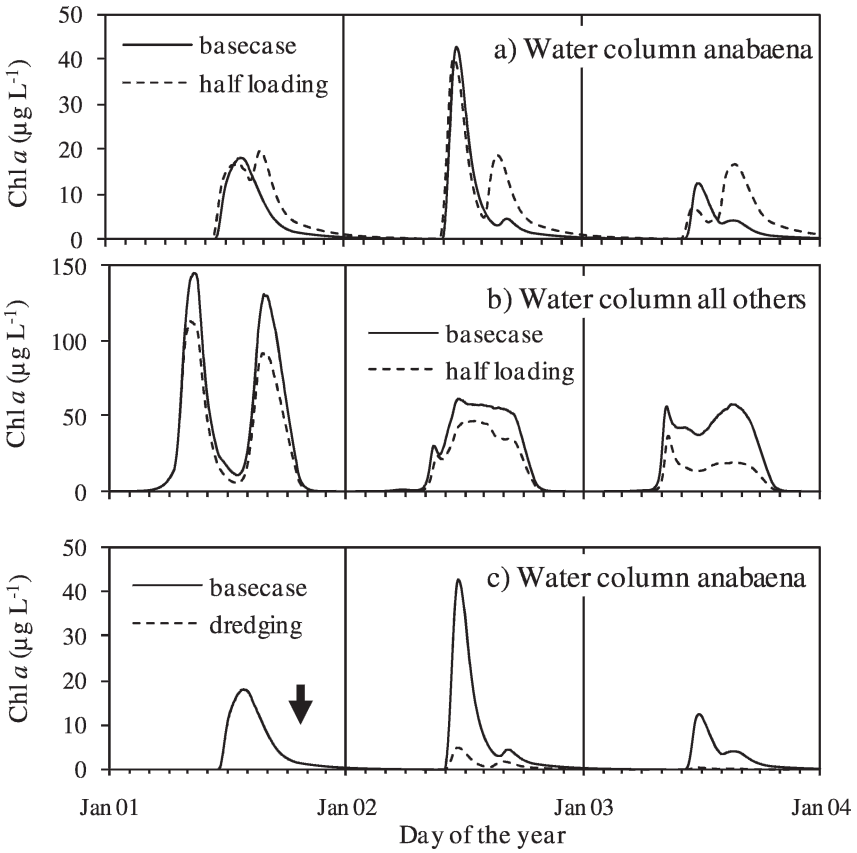

Fig. 8. Management scenarios. (a, b) Nutrient input is halved. Chlorophyll *a* for *Anabaena* and all other species are shown. *See* Fig. 3 legend for conversion. (c) Model simulation to investigate the effect of reducing the sediment akinete density. Sediment akinete density was reduced by 90% toward the end of year 1 (*see* arrow).

and internal (e.g., alum precipitation, sediment dredging) nutrient loading reduction, N : P ratio manipulation, mechanical mixing, increased flushing, biomanipulation, and others (Chorus and Mur 1999; Paerl et al. 2001). Here, we use the model to evaluate two management scenarios. First, since P levels are generally expected to favor cyanobacteria, especially nitrogen fixers, like *Anabaena* (Paerl et al. 2001; Downing et al. 2001), a potential management action is to reduce the external P loading. However, a simulation with half the nutrient input predicts that *Anabaena* densities increase compared with the base case (Fig. 8a). *Anabaena* are less sensitive to the decrease in water column concentration because their predominant nutrient source is the sediment bed. Other phytoplankton species, however, decrease (Fig. 8b), which increases light availability for *Anabaena* and increases their productivity. Of course, this simulation neglects numerous other indirect effects (e.g., response of zooplankton, other nutrients), but it highlights the importance of the resting stage and resulting complexity of the population response to change. The second management scenario investigated involves reducing the sediment seed source. One approach is sediment removal, which has the advantage of removing sediment bed akinetes and phosphorus, a source of internal loading, but the disadvantage of being relatively expensive and a temporary solution. Another option is to drain the reservoir periodically for drying of sediments. Baker and Bellifemine (2000) found rapid loss of viability and abundance of akinetes of *Anabaena circinalis* in sediments as a result of desiccation. To investigate the effect of reducing the sediment bed akinete density, we performed a simulation where the akinete density in the sediment bed is reduced toward the end of year 1. A removal efficiency of 90%, corresponding to 0.06×10^6 cells cm^{-2} after removal, was simulated. According to the model (Fig. 8c), there is a direct relationship between water column bloom size and sediment akinete density for *Anabaena* in Bugach Reservoir. The model can be used to predict what the concentration in years 2 and 3 would have been following the removal. Predictions of future conditions will be more uncertain because of changing physical and ecological (i.e., higher trophic levels) conditions.

Discussion

Ecology of resting stage formation and management implications—The life cycle of many phytoplankton species includes a resting stage. Although the resting stage cells can be observed relatively easily, understanding their purpose is more difficult. Do they prevent washout or predation during unfavorable growth condition? Or is it a mechanism of nutrient uptake from the sediment bed? Both? How does

this feature affect the response of the population to changing conditions? This study used a model to gain insights into the ecology of *Anabaena* akinete formation in Bugach Reservoir, which may be applicable to other species and locations. The formation of resting stages is an important feature of *Anabaena,* which is required for survival on an annual basis. Through this life cycle stage, the majority of the population overwinters in the sediment bed and most of the nutrient uptake occurs in the sediment bed. This latter feature is especially important from a management perspective. Since the *Anabaena* population gets most of its nutrients from the sediment bed, it will be less sensitive to changes in water column nutrient concentrations, as may result from external load reductions. Further, since other species would be affected by the nutrient reduction, other resources (i.e., light) may increase. Therefore, reducing external nutrient inputs would, at least in the short term, increase *Anabaena* densities in Bugach Reservoir. It may do the same for other resting stage-forming phytoplankton in other lakes or reservoirs.

Utility of the agent-based approach—The utility of numerical simulation models as management and research tools is well established. In a management context, they allow us to quantitatively relate stressors (e.g., nutrient input) to system response (e.g., trophic state). For research, they can be used for hypothesis testing by performing numerical (in silico) experiments. More specifically, models constitute a tool for linking observations from laboratory and field scales, and they can be used to answer questions like "is the germination rate observed in laboratory experiments consistent with field observations?" As our understanding of aquatic microorganisms increases, so does our appreciation for their complexity and the need to capture it in models. In spatially structured habitats, different life histories lead to intrapopulation variability in properties and behavior. Theoretically, these features can be captured using agent-based or traditional population-level models, and the pros and cons of either approach will likely be debated for some time. We believe that the agent-based approach is well suited for constructing this next generation of phytoplankton models, and the *Anabaena* model presented here demonstrates the utility of the approach. Additional features, including more complex biochemistry and explicit consideration of heterocysts, are straightforward to implement with the agent-based approach (from a programming perspective). However, maybe the strongest argument for the agent-based approach comes from the history of modeling of higher trophic levels. There, population-level models (i.e., Lotka-Volterra) were originally developed. Then, as the importance of complexity and adaptive behavior was increasingly recognized and computing limitations diminished, the popularity of agent-based modeling increased. With an increased realization and understanding of the complexity of microorganisms and further advances in computing technology, we should see phytoplankton modeling follow this trend over the next decade. We anticipate that agent-based modeling will become widespread and an integral component of research and management in this area.

Simulation of akinete differentiation and germination—Most processes (e.g., photosynthesis, nutrient uptake) were implemented in the model using established equations. The major new feature is the explicit consideration of the akinete resting stage. During the model development, the literature on akinete differentiation and germination was reviewed in detail, which showed that numerous factors can affect these transitions. However, the present knowledge is insufficient to construct a detailed mechanistic model, and we therefore opted to keep the model simple. A vegetative cell differentiates to an akinete when the growth conditions decline and germinates back to a vegetative cell when the growth conditions improve. The actual mechanisms of these processes are undoubtedly more complicated. However, despite this simplified approach, the model is able to capture the main features of the data. We also expect that the simplified form of the model may make it more applicable to other species. In the future, as more information on these processes becomes available, we expect that this model will be modified. This is similar to the way modeling of other processes has evolved. Nutrient uptake, for example, was first simulated using simple Michaelis–Menten representation, and later modified to incorporate the effect of internal nutrients and other factors.

References

Adams, D. G., and P. S. Duggan. 1999. Transley review no. 107. Heterocysts and akinete differentiation in cyanobacteria. New Phytol. **144:** 3–33.

Baker, P. D. 1999. Role of akinetes in the development of cyanobacterial populations in the lower Murray River, Australia. Mar. Freshw. Res. **50:** 265–279.

———, and D. Bellifemine. 2000. Environmental influences on akinete germination of *Anabaena circinalis* and implications for management of cyanobacterial blooms. Hydrobiologia **427:** 65–73.

Barbiero, R. P., and J. Kann. 1994. The importance of benthic recruitment to the population development of *Aphanizomenon flos-aquae* and internal loading in a shallow lake. J. Plankton Res. **16:** 1581–1588.

———, and E. B. Welch. 1992. Contribution of benthic blue-green algal recruitment to lake populations and phosphorus translocation. Freshw. Biol. **27:** 249–260.

Bortleson, G. C., and G. F. Lee. 1974. Phosphorus, iron, and manganese distribution in sediment cores of six Wisconsin lakes. Limnol. Oceanogr. **19:** 794–801.

Chapra, S. C. 1997. Surface water-quality modeling. McGraw-Hill.

Chorus, I., and L. Mur. 1999. Preventative measures, p. 235–273. *In* I. Chorus and J. Bartram [eds.], Toxic cyanobacteria in water. Taylor and Francis.

Daley, B. 2006. Toxic algae levels feared in lower Charles River. Boston Globe.

Di Toro, D. M. 1978. Optics of turbid estuarine waters: Approximations and applications. Water Res. **12:** 1059–1068.

Downing, J. A., S. B. Watson, and E. McCauley. 2001. Predicting cyanobacteria dominance in lakes. Can. J. Fish. Aquat. Sci. **58:** 1905–1908.

Droop, M. R. 1968. Vitamin B_{12} and marine ecology. IV. The kinetics of uptake, growth and inhibition in *Monochrysis lutheri*. J. Mar. Biol. Assoc. UK **48:** 689–733.

Fay, P. 1969*a*. Metabolic activities of isolated spores of *Anabaena cylindrica*. J. Exp. Bot. **20:** 100–109.

———. 1969*b*. Cell differentiation and pigment composition in *Anabaena cylindrica*. Arch. Microbiol. **67:** 62–70.

———. 1988. Viability of akinetes of the planktonic cyanobacterium *Anabaena circinalis*. Proc. R. Soc. Lond. B **234:** 283–301.

———, J. A. Lynn, and S. C. Majer. 1984. Akinete development in the planktonic blue-green alga *Anabaena circinalis*. Br. Phycol. J. **19:** 163–173.

Grimm, V., and others. 2006. A standard protocol for describing individual-based and agent-based models. Ecol. Model. **198:** 115–126.

Head, R. M., R. I. Jones, and A. E. Bailey-Watts. 1999*a*. Vertical movements by planktonic cyanobacteria and the translocation of phosphorus implications for lake restorations. Aquat. Conserv. Mar. Freshw. Ecosyst. **9:** 111–120.

———, ———, and ———. 1999*b*. An assessment of the influence of recruitment from the sediment on the development of planktonic populations of cyanobacteria in a temperate mesotrophic lake. Freshw. Biol. **41:** 759–769.

Healey, F. P. 1982. Phosphate, p. 105–124. *In* N. G. Carr and B. A. Whitton [eds.], The biology of cyanobacteria. Univ. California Press.

Hellweger, F. L. 2008. Spatially explicit individual-based modeling using a fixed super-individual density. Comput. Geosci. **34:** 144–152.

———, K. J. Farley, U. Lall, and D. M. Di Toro. 2003. Greedy algae reduce arsenate. Limnol. Oceanogr. **48:** 2275–2288.

———, and E. Kianirad. 2007. Accounting for intra-population variability in biogeochemical models using agent-based methods. Environ. Sci. Technol. **41:** 2855–2860.

———, and U. Lall. 2004. Modeling the effect of algal dynamics on arsenic speciation in Lake Biwa. Environ. Sci. Technol. **38:** 6716–6723.

Hense, I., and A. Beckmann. 2006. Toward a model of cyanobacteria life cycle—effects of growing and resting stages on bloom formation of N_2-fixing species. Ecol. Model. **195:** 205–218.

Howard, A. 2001. Modeling the movement patterns of the cyanobacterium *Microcystis*. Ecol. Appl. **11:** 304–310.

HydroQual. 1998. A water quality model for Jamaica Bay: Calibration of the Jamaica Bay Eutrophication Model (JEM). HydroQual.

———. 2001. Addendum to: Bays Eutrophication Model (BEM): Modeling analysis for the period 1992–1994. HydroQual.

Kalachova, G. S., A. A. Kolmakova, M. I. Gladyshev, E. S. Kravchuk, and E. A. Ivanova. 2004. Seasonal dynamics of amino acids in two small Siberian reservoirs dominated by prokaryotic and eukaryotic phytoplankton. Aquat. Ecol. **38:** 3–15.

Karlsson, I. 2003. Benthic growth of *Gloeotrichia echinulata* cyanobacteria. Hydrobiologia **506–509:** 189–193.

Karlsson-Elfgren, I., and A.-K. Brunberg. 2004. The importance of shallow sediments in the recruitment of *Anabaena* and *Aphanizomenon* (cyanophyceae). J. Phycol. **40:** 831–836.

Kravchuk, E. S., E. A. Ivanova, and M. I. Gladyshev. 2006. Seasonal dynamics of akinetes of *Anabaena flos-aquae* in bottom sediments and water column of small Siberian reservoir. Aquat. Ecol. **40:** 325–336.

Kreft, J.-U., G. Booth, and J. W. T. Wimpenny. 1998. BacSim, a simulator for individual-based modelling of bacterial colony growth. Microbiology **144:** 3275–3287.

Lee, D.-Y., and G.-Y. Rhee. 1999. Kinetics of growth and death in *Anabaena flos-aquae* (cyanobacteria) under light limitation and supersaturation. J. Phycol. **35:** 700–709.

Lung, W. S., and H. W. Paerl. 1988. Modeling blue-green algal blooms in the Lower Neuse River. Water Res. **22:** 895–905.

McGillicuddy, D. J., Jr., D. M. Anderson, D. R. Lynch, and D. W. Townsend. 2005. Mechanisms regulating large-scale seasonal fluctuations in *Alexandrium fundyense* populations in the Gulf of Maine: Results from a physical–biological model. Deep-Sea Res. II **52:** 2698–2714.

Morel, F. M. M. 1987. Kinetics of nutrient uptake and growth in phytoplankton. J. Phycol. **23:** 137–150.

Nichols, J. M., D. G. Adams, and N. G. Carr. 1980. Effect of canavanine and other amino acid analogues on akinete formation in the cyanobacterium *Anabaena cylindrica*. Arch. Microbiol. **127:** 67–75.

Oh, H.-M., J. Maeng, and G.-Y. Rhee. 1991. Nitrogen and carbon fixation by *Anabaena* sp. isolated from a rice paddy and grown under P and light limitations. J. Appl. Phycol. **3:** 335–343.

Olli, K., K. Kangro, and M. Kabel. 2005. Akinete production of *Anabaena lemmermannii* and *A. cylindrica* (Cyanophyceae) in natural populations of N- and P-limited coastal mesocosms. J. Phycol. **41:** 1094–1098.

Paerl, H. W. 1988. Nuisance phytoplankton blooms in coastal, estuarine and inland waters. Limnol. Oceanogr. **33:** 823–847.

———, R. S. Fulton, III, P. H. Moisander, and J. Dyble. 2001. Harmful freshwater algal blooms with an emphasis on cyanobacteria. Sci. World **1:** 76–113.

Pandey, K. D., and A. K. Kashyap. 1987. Factors affecting formation of spores (Akinetes) in cyanobacterium *Anabaena doliolum* (Ads strain). J. Plant Physiol. **127:** 123–134.

Pascual, M., and H. Caswell. 1997. From the cell cycle to population cycles in phytoplankton-nutrient interactions. Ecology **78:** 897–912.

Pettersson, K., E. Herlitz, and V. Istvanovics. 1993. The role of *Gloeotrichia echinulata* in the transfer of phosphorus from sediments to water in Lake Erken. Hydrobiologia **153:** 123–129.

Prokopkin, I. G., V. G. Gubanov, and M. I. Gladyshev. 2006. Modelling the effect of planktivorous fish removal in a reservoir on the biomass of cyanobacteria. Ecol. Model. **190:** 419–431.

Rai, A. K., and G. P. Pandey. 1981. Influence of environmental stress on the germination of *Anabaena vaginicola* akinetes. Ann. Bot. **48:** 361–370.

Rao, V. V., R. Ghosh, and H. N. Singh. 1987. Diazotrophic regulation of akinete development in the cyanobacterium *Anabaena doliolum*. New Phytol. **106:** 161–168.

Reynolds, C. S. 1972. Growth, gas vacuolation and buoyancy in a natural population of a planktonic blue-green alga. Freshw. Biol. **2:** 87–106.

Rhee, G.-Y., and T. C. Lederman. 1983. Effects of nitrogen sources on P-limited growth of *Anabaena flos-aquae*. J. Phycol. **19:** 179–185.

Rigler, F. H. 1964. The phosphorus fractions and the turnover time of inorganic phosphorus in different types of lakes. Limnol. Oceanogr. **9:** 511–518.

Scheffer, M., J. M. Baveco, D. L. Deangelis, and K. A. Rose. 1995. Super-individuals: A simple solution for modelling large populations on an individual basis. Ecol. Model. **80:** 161–170.

Shuter, B. J. 1978. Size dependence of phosphorus and nitrogen subsistence quotas in unicellular microorganisms. Limnol. Oceanogr. **23:** 1248–1255.

Smith, R. E. H., and J. Kalff. 1982. Size-dependent phosphorus uptake kinetics and cell quota in phytoplankton. J. Phycol. **18:** 275–284.

Sommer, U. 1998. Biologische meereskunde. Springer.

Tang, E. P. Y., R. Tremblay, and W. F. Vincent. 1997. Cyanobacterial dominance of polar freshwater ecosystems: Are high-latitude mat-formers adapted to low temperature? J. Phycol **33:** 171–181.

Thingstad, T. F. 1987. Utilization of N, P, and organic C by heterotrophic bacteria. I. Outline of a chemostat theory with a consistent concept of ''maintenance'' metabolism. Mar. Ecol. Prog. Ser. **35:** 99–109.

Thomann, R. V., and J. A. Mueller. 1987. Principles of surface water quality modeling and control. Harper Collins.

Vadstein, O., A. Jensen, Y. Olsen, and H. Reinertsen. 1988. Growth and phosphorus status of limnetic phytoplankton and bacteria. Limnol. Oceanogr. **33:** 489–503.

van Dok, W., and B. T. Hart. 1996. Akinete differentiation in *Anabaena circinalis* (Cyanophyta). J. Phycol. **32:** 557–565.

Vanderploeg, H. A., J. R. Leibig, W. W. Carmichael, A. A. Agy, T. H. Johengrn, G. L. Fahnenstiel, and T. F. Nalepa. 2001. Zebra mussel (*Dreissena polymorpha*) selective filtration promoted toxic Microcystis blooms in Saginaw Bay (Lake Huron) and Lake Erie. Can. J. Fish. Aquat. Sci. **58:** 1208–1221.

Verspagen, J. M. H., E. O. F. M. Snelder, P. M. Visser, K. D. Jöhnk, B. W. Ibelings, L. R. Mur, and J. Huisman. 2005. Benthic–pelagic coupling in the population dynamics of the harmful cyanobacterium *Microcystis*. Freshw. Biol. **50:** 854–867.

[WDNR] Wisconsin Department of Natural Resources. 1989. Wisconsin Department of Natural Resources environmental impact statement—Delavan Lake rehabilitation project. Wisconsin Department of Natural Resources.

Westwood, K. J., and G. G. Ganf. 2004. Effect of cell flotation on growth of *Anabaena circinalis* under diurnally stratified conditions. J. Plankton Res. **26:** 1183–1197.

Wetzel, R. G. 2001. Limnology: Lake and river ecosystems, 3rd ed. Academic.

Woods, J. D. 2005. The Lagrangian ensemble metamodel for simulating plankton ecosystems. Prog. Oceanogr. **67:** 84–159.

Yamamoto, T., T. Seike, T. Hashimoto, and K. Tarutani. 2002. Modeling the population dynamics of the toxic dinoflagellate *Alexandrium tamarense* in Hiroshima Bay, Japan. J. Plankton Res. **24:** 33–47.

Received: 19 October 2007
Accepted: 28 February 2008
Amended: 10 March 2008